



Intralesional cryosurgery enhances the involution of recalcitrant auricular keloids: a new clinical approach supported by experimental studies

Yaron Har-Shai, MD^{1,2}; Edmond Sabo, MD³; Ewa Rohde, MD^{1,4}; Michael Hyams, MD²; Chalid Assaf, MD¹; Christos C. Zouboulis, MD^{1,5}

1. Department of Dermatology, Charité University Medicine Berlin, Campus Benjamin Franklin, Berlin, Germany

2. Department of Plastic Surgery, Linn Medical Center, The Bruce Rappaport Faculty of Medicine, Technion – Israel Institute of Technology, Haifa, Israel

3. Department of Pathology, Carmel Medical Center, The Bruce Rappaport Faculty of Medicine, Technion – Israel Institute of Technology, Haifa, Israel

4. Institute for Medical and Technical Physics and Laser Medicine, Berlin, Germany, and

5. Departments of Dermatology and Immunology, Dessau Medical Center, Dessau, Germany

Reprint requests

Prof. Dr. Christos C. Zouboulis,
Departments of Dermatology and
Immunology, Dessau Medical Center,
Auenweg 38, 06847 Dessau, Germany.
Fax: +49 340 5014025; email:
christos.zouboulis@klinikum-dessau.de

Manuscript received: October 10, 2004

Accepted in final form: July 18, 2005

DOI:10.1111/j.1743-6109.2005.00084.x

ABSTRACT

To explain the mechanism of action of a novel intralesional cryoprobe, thermal behavior measurements, and histological studies were performed in swine muscle specimens after intralesional cryosurgery *ex vivo*. Slow cooling (20 °C/min) and thawing (25 °C/min) rates, end temperature of –30 °C, produced 8 mm wide diffuse coagulative-type necrosis and a 3 mm-wide transition zone around the cryoprobe. In contrast, contact cryosurgery showed fast cooling and thawing rates (80 °C/min) and an end temperature of –100 °C. Efficacy and safety of the intralesional cryoprobe was further assessed in ten recalcitrant auricular keloids in nine Caucasian patients. There was a 67.4 ± 23 percent reduction of scar volume at the end of the 18-month follow-up period after a single intralesional treatment ($p < 0.005$). Significant reduction of hardness, elevation, and redness as well as itching, pain, and tenderness was documented. The histomorphometric analysis, including spectral and fractal analysis, as well as assessment of the fast Fourier transform algorithm, showed parallel alignment and reorganization of the collagen fibers in the treated scar similar to that in the normal dermis. A long hold time in the deep scar core caused minimal damage to the superficial tissue, including melanocytes. There was no evidence of permanent hypopigmentation, active bleeding, infection, or recurrence. The major advantages of the intralesional cryoprobe, including the marked efficacy of a single treatment, may have a major importance in the clinical application of cryosurgery in the treatment of keloids and of other lesions localized deep in the skin.

Hypertrophic scars and keloids are benign, fibrous proliferations that exhibit high recurrence rates of 55–100 percent following surgical excision.^{1–4} The incidence of auricular keloids following ear piercing has been estimated at 2.5 percent in the patients of an American teaching hospital.⁵ Lobular scarring is the fifth most common reason for adult and pediatric dermatology consultations in a survey of black patients attending a London hospital.⁶ It was documented that auricular keloids develop more frequently on the posterior aspect of the lobule than on its anterior surface.⁷ A family genetic predisposition to the formation of keloids has been described.⁸

The increasing trend for cosmetic piercing, and for multiple ear piercing, especially among youngsters, and bearing in mind that the incidence of keloid formation is likely to be higher during times of hyperactivity of the pituitary gland, such as puberty and pregnancy,^{9,10} suggest that auricular keloids will become a more frequent part of dermatological and plastic surgery practices.

The etiology for auricular keloids is diverse and includes piercing,¹¹ trauma and skin lacerations, burns, surgical interventions such as skin-tumor excision, correction of con-

genital ear deformations such as lop ears, infections, contact dermatitis such as allergy to earrings containing nickel. The developing auricular keloids vary considerably in size. They are usually relatively small but large lesions might weigh up to 38 g.¹² Auricular keloids may cause a permanent and significant distress to the patient as well as daily disability in wearing eyeglasses or sleeping on the side of the affected ear.

Despite recent advances in the understanding of wound healing and scar formation treatment of hypertrophic scars and keloids is still a challenging problem. A variety of treatments have been described for overcoming the high recurrence rates with varying degrees of success ranging from 0 to 100 percent.¹³ These include conservative methods such as massage, use of silicone gel sheets and earring splints⁴; minimally invasive methods including intralesional corticosteroid, verapamil,² or interferon injections,

FFT Fast fourier transformation
H&E Hematoxylin and eosin

cryosurgery and/or laser therapy. Surgical interventions such as excision, keloid core, or subtotal excision,^{14,15} which may be followed by reconstruction with a split or full-skin graft, local flap,¹⁶ and immediate radiation therapy,^{17–19} and postoperative systemic administration of corticosteroids¹¹ have been proposed.

It was postulated that auricular keloids are more difficult to treat than those at other sites, with a higher rate of failure and/or recurrence.¹⁷ In addition, it is more difficult to excise a helical keloid completely and to achieve primary skin closure than at many other body sites without causing tension and disfigurement.

Cryosurgery as a monotherapy regimen for the management of hypertrophic scars and keloids was introduced in 1982 by Shepherd and Dawber.²⁰ Mende,²¹ Zouboulis and Orfanos,²² and others showed that repeated contact/spray cryosurgical sessions can have a beneficial effect on the lesions with 68–81 percent remission rates and rare recurrences (2%). However, 1–20 monthly sessions using surface cryosurgery are required to achieve these results.

Recently, intralesional cryosurgery using liquid nitrogen and a 20 G injection needle^{23–25} or multiple 18 G injection needles²⁶ or an intralesional cryoprobe²⁷ were introduced to treat hypertrophic scars and keloids. This cooperative study was designed by two of the centers initially involved to assess efficacy and safety of the intralesional cryoprobe in the treatment of difficult indications, such as recalcitrant auricular keloids, and to explain its mechanism of action.

MATERIALS AND METHODS

Thermal behavior measurements were made *in vitro* and on a fresh swine muscle model using thermocouples to evaluate the thermal history and injury mechanisms of the intralesional-cryosurgery technique as compared with the contact-cryosurgery method. In addition, punch biopsies from the central area of the frozen tissue were taken for histological examinations following standard techniques.

Cryoprobe characteristics and calibration

To evaluate the possible mechanisms of injury during intralesional cryosurgery, the thermal history of the isolated intralesional cryoprobe was examined at room temperature. The data gathered were compared with 10 mm diameter round contact cryoprobes (ERBE, Tübingen, Germany), which are in common use for the treatment of hypertrophic scars and keloids.²⁸ The isolated thermal histories of these cryoprobes including freezing rate, end temperature, hold time, and thawing rate were evaluated by NiCr–Ni thermocouples (temperature drift of 0.01%) which were connected to a GTH 1160 digital quick response thermometer (Greisinger, Regenstauf, Germany). The three thermocouple-thermometers showed an identical room temperature before initiating the experiments. The cooling time was tested during 180 seconds and the thawing phase was traced for another 240 seconds.

Thermal history in an *ex vivo* swine model

The thermal history was determined *ex vivo* in a fresh swine gluteal muscle. This tissue resembles keloids, which

are mainly composed of a collagenous structure, and it was chosen because of the ability to precisely locate by ultrasonography the depth of the intralesional cryoneedle position during all experiments as well as to enable us to measure the temperature history on a similarly homogeneous tissue without alterations in tissue consistency, similar to those existing in a healthy skin. Following the introduction of the cryoprobe into the muscle at a 6 mm depth, which was confirmed by ultrasonography, three thermocouples were introduced to evaluate the thermal history during and after the intralesional freezing process. One thermocouple approached the intralesional needle while the other two thermocouples were situated 3 mm toward the surface and on the muscle's surface, respectively. The measurements of the contact probe consisted of three thermocouples but in a reverse placement. One thermocouple abutted the surface of the probe, which was applied onto the muscle surface, while the second and third thermocouples were placed at a depth of 3 and 6 mm from the surface, respectively.²⁹ Thereafter, the cryoprobe was connected to the cryogun. Following the initiation of the freezing process, the temperature changes of each thermocouple were recorded every 15 seconds. After 720 seconds of cooling time, the freezing process was stopped and the thawing time was recorded for another 360 seconds. With the contact probe, the cooling time had a duration of 360 seconds with a thawing period of 720 seconds. All captured data were placed into an Excel spreadsheet program.

Patients and lesions for pilot clinical studies

Nine Caucasian patients (seven females and two males) aged from 18 to 55 years with a total of 10 auricular keloids (6 months–6-year-old) signed an informed consent form and were included in a pilot study. The etiology of the lesions were piercing (9/10) and skin laceration (1/10) with their location lobular (7/10), or helical (3/10). Previous scar treatment included surgical excisions, laser surgery, surface (contact/spray) cryosurgery, intralesional corticosteroid injections, and local application of silicone ointments was without improvement. The medical history revealed hypertension and diabetes in one patient aged 55 years and asthma in a 46-year-old patient.

Intralesional cryoprobe

A novel intralesional cryoprobe (European Patent Number 1299043; US Patent Number 6,503,246; 27) with an elongated double-lumen uninsulated needle with a cryogen vent and a sharp-cutting, sealed, distal tip to easily penetrate the hard, rubbery, and dense keloids was used in the study. The cryoprobe was reused after autoclave sterilization. The proximal end of the cryoprobe was attached to an adaptor, which was connected to a “cryogun” cryogen source, forcing liquid nitrogen to circulate through the needle produces an ice ball around the cryoneedle, which can freeze the adjacent tissue.

Clinical trial protocol

The trial, which extended over an 18-month period, evaluated the volume reduction of the keloids. Imprints were made with Elite H-D Putty Vinyl polysiloxane

high-precision (>99.5%) impression material (Zhermack, Badia Polesine, Italy) and a water displacement method was used 6, 12, and 18 months before and after a single intralesional cryosurgery session. In addition objective parameters (hardness, elevation, and redness) and subjective complaints (itching, pain, and tenderness) were examined on a scale of 0 (none) to 3 (maximum). The assessments were performed before treatment and at weeks 1 and 2 and months 1, 2, 3, 6, 12, and 18 after treatment. Photographs were taken before and 18 months after treatment.

Method of treatment

After the patient was placed in a supine position, the skin surface of the keloid was cleaned with disinfectant solution and draped. The area of penetration into the scar and the underlying subcutaneous tissue was anesthetized locally with lidocaine 1 percent. The sterile cryoprobe was forced into the long axis of the scar until the sharp tip of the needle penetrated the opposite distal edge of the scar, thus maximizing the volume of scar to be frozen. Attention was taken to prevent any penetration of the cryoprobe into uninvolved surrounding skin. Sterile gauze pads were placed under the proximal and distal parts of the cryoprobe and care was taken to assure that the vent nostril was positioned away from the patient to prevent accidental freezing of uninvolved skin.

The proximal part of the probe was connected via a luer lock to the cryogun (Brymill Cryogenic Systems, Ellington, CT; Premier Medical Products, Plymouth Meeting, PA), which was filled about 10–15 minutes beforehand with liquid nitrogen to allow a sufficient pressure to build-up inside the cryogun. By activating the cryogun trigger, the valve opened and the cryogen entered the cryoprobe under a pressure of approximately 5 pounds per square inch, thereby freezing the keloid. A forced steam of the liquid nitrogen gas flowed out from the vent nostril during the entire freezing process. Two iceballs appeared shortly at the two cryoprobe penetration sites and with time they gradually spread toward each other until complete freezing of the keloid was achieved. Following a complete freezing of the keloid, regardless of the duration of the cryosurgery process, the cryogun trigger was released to stop the freezing and the cryoprobe was left to thaw for 1–2 minutes and was then withdrawn. After a complete thawing of the keloid, slight bleeding from the penetration points of the probe required the application of a sterile dressing. The patients were instructed to wash the treated scar daily and to apply an antibiotic ointment until full recovery of the treated scar was accomplished.

Histomorphometric studies in human tissue

Punch biopsies for histomorphometric evaluation including spectral and fractal analysis as well as fast Fourier transformation (FFT) algorithm, were taken from eight scars before treatment and after 6 months after the single cryosurgical session (Figure 1). To maintain specimen orientation a marking ink was applied with respect to the cryoprobe axis. After treatment, the tissue was immediately fixed in 10 percent neutral-buffered formalin. Three micrometer-thick sections were obtained and stained by hematoxylin and eosin (H&E). The area of cryosurgical

damage was assessed and measured with a scaled ocular micrometer ($\times 100$ magnification). The radii of the complete and partial injury zones were measured perpendicular to the cryoprobe axis. Vascular injury was also histologically evaluated.

Spectral computerized morphometric analysis

Deparaffinized keloid biopsy tissue sections were histochemically stained with picrosirius red and examined by polarization microscopy.^{27,30,31} Staining of collagen matrix revealed a mixture of red and green fibers of different proportions according to the particular spatial orientation levels. The red-stained fibers represent mature thick and tightly packed collagen fibers and the green-stained fibers represent young thin and loosely spaced collagen fibers. The ratio of red to green staining represents the relative amount of the two types of collagen fibers. Images were captured by a Sony trichip video camera (Tokyo, Japan) connected to an Olympus light microscope (Tokyo, Japan) and digitized with the aid of a frame grabber and an IBM-compatible personal computer equipped with a 17 in. high-resolution screen. Spectral computerized morphometric analysis of the collagen fibers was then performed using the Image Pro Plus 4.5 software (MediaCybernetics, Carlsbad, CA). Ten representative microscopic fields were scanned at a $\times 10$ magnification. After establishment of the appropriate thresholds, the relative areas of green and red collagen fibers were stained separately and calculated by the program. Then, the average green-to-red ratio was computed for each scar.

Fast Fourier transformation

The orientation index of the collagen fibers in the keloid biopsy tissue sections before and after cryosurgery was evaluated using the FFT algorithm.^{32–34} To compute the orientation index, the Auto-Pro environment of the Image Pro Plus 4.5 software was used. A macro-algorithm was developed that automatically traces thickness, and singles out the longest diameter of the fibers. Subsequently, the FFT algorithm was applied to obtain two-dimensional power-scatter grams of the histological images. A median filter was applied to homogenize close pixels. A scar with randomly oriented collagen fibers exhibited a circular scatter gram, compared with a scar with well-oriented fibers, which showed an elongated (elliptically shaped) scatter gram. The orientation index is equivalent to the calculated ratio, between the maximal and the minimal diameters of the scatter gram provided by the FFT algorithm. The larger the index value, the greater the degree of collagen fiber orientation in the scar.

Fractal analysis of collagen fibers

The image fractal geometry of the collagen fibers before and after treatment was calculated using the box-counting method.^{35,36} This method allows for the determination of fractal dimension of both scale invariant and self-similar structures. To estimate the box dimension, the Euclidean space containing the images is divided into a grid of boxes of size "s." Then, the size "s" was changed to progressively smaller sizes, and the corresponding number of nonempty

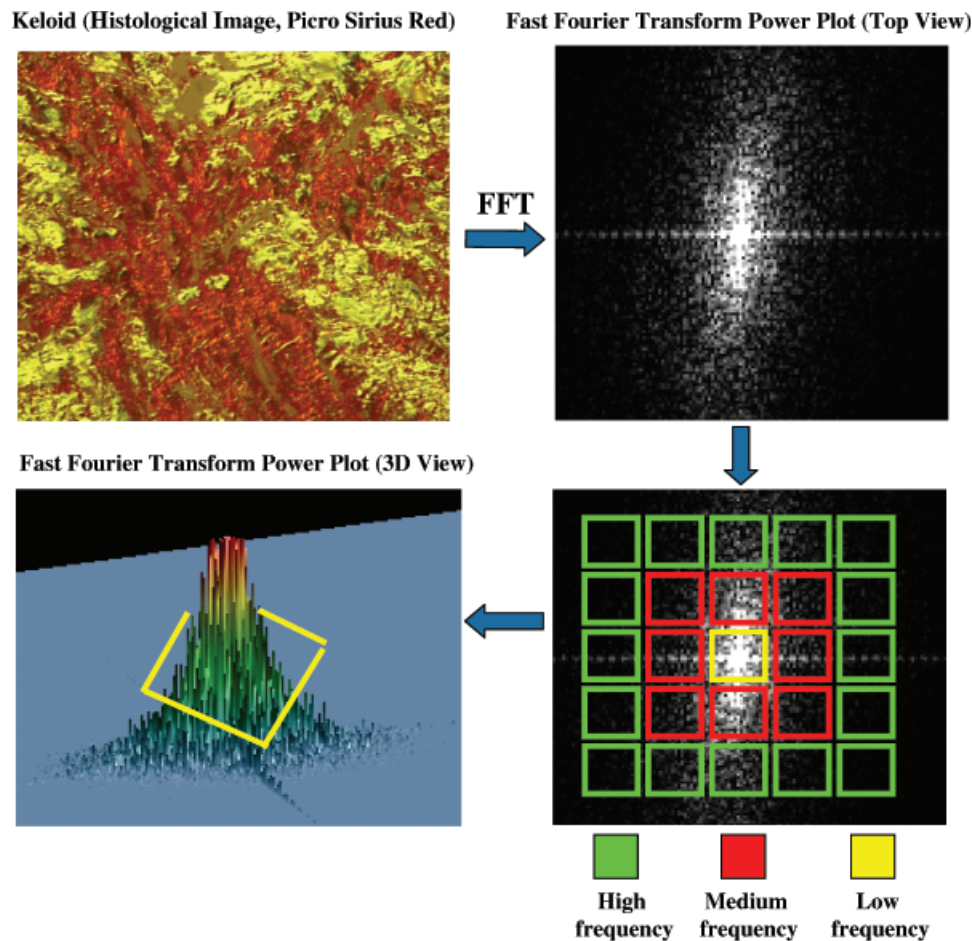


Figure 1. Schematic representation of the consecutive steps to achieve a 3D histomorphological fractal analysis power plot. The tissue is stained with picrosirius red, followed by performing the fast Fourier transform power plot algorithm which is then plotted on a box-counting grid. This enables one to construct the 3D fractal power plot view.

boxes was counted. The fractal dimension values range between 1 and 2. For classical geometric shapes such as a line, a square and a cube, the fractal dimension is identical to the classic (Euclidean) dimension, being 1 for the line, 2 for square, and 3 for a cube. However, a geometrical structure with complex contour is best represented by fractal dimension i.e., a rational number. The more complex the contour, the larger is the fractal dimension. In our study, the fractal dimension reflected the level of architectural complexity of the keloid microscopic images. The mean values of the fractal dimensions of all of the fields analyzed per case were used for statistical evaluation.

Statistical analysis

Statistical analysis was executed using the SPSS vs10 program (SPSS, Inc., Chicago, IL). The data were analyzed for sample normality using the Kolmogorov–Smirnov test. The mean value and standard error of the mean were calculated and presented for each group. The clinical scores, the scar volumes, the red to green ratios, the orientation index and the fractal dimension obtained before and after

cryosurgery were compared using the Wilcoxon test for paired observations. Two-tailed values of $p \leq 0.05$ were considered to be statistically significant.

RESULTS

The thermal history of the isolated intralesional cryoprobe showed a fast cooling rate (200 °C/min). The end temperature was shown to be –196 °C, which was achieved after 60 seconds and remained at this low level for another 120 seconds (hold time). The thawing rate was equally fast, i.e., the temperature returned from approximately –200 °C to almost 0 °C (200 °C/min) after 60 seconds (Figure 2A). The surface cryoprobe also exhibited a fast cooling rate (160 °C/min), i.e., the probe temperature was –136 °C after 60 seconds, which remained constant until 180 seconds. The thawing rate, however, was very slow (40 °C/min), i.e., the probe temperature was –35 °C at 420 seconds.

The *ex vivo* studies in the swine muscle revealed a completely different thermal behavior. The intralesional cryoprobe showed a much slower cooling rate (20 °C/min) with an end temperature of –30 °C. However, the thawing

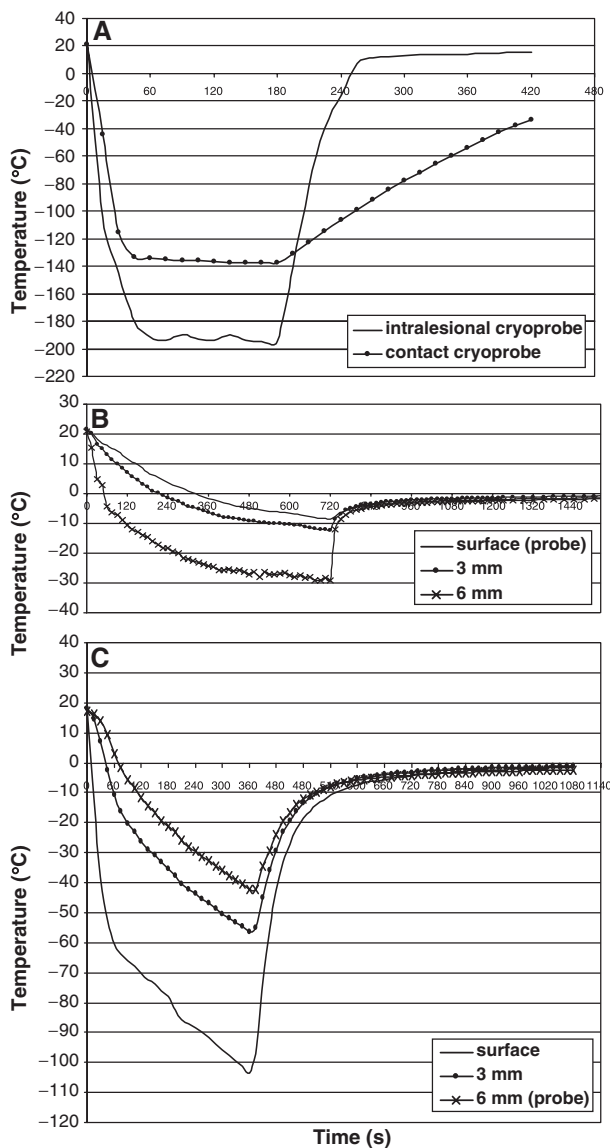


Figure 2. Thermal profiles at different locations within the lesion and on the skin surface. (A) Thermal history of the isolated intralesional cryoprobe with comparison to the contact cryoprobe. (B) Temperatures recorded by the thermocouples during the ex vivo intralesion cryosurgery at the surface, and in the tissue at depths of 3 and 6 mm (location of the cryoprobe) and (C) during the ex vivo contact cryosurgery (location of the cryoprobe) and in the tissue at depths of 3 and 6 mm.

rate was faster (35 °C/min). The 3 mm and surface thermocouples showed a slower cooling rate (5 °C/min), end temperature of -12 °C with a long constant holding time and a faster thawing rate (8 °C/min; Figure 2B). The contact probe showed fast cooling and thawing rates (80 °C/min) with an end temperature of -100 °C and without a constant hold time. The 3 and 6 mm deep thermocouples showed a similar pattern, i.e., faster cooling (20 °C/min) and thawing (25 °C/min) rates when compared with the intralesional method, with almost no hold time

and an end temperature of -58 and -42 °C, respectively (Figure 2C).

Histological studies

Histologically, the frozen swine muscle showed cryolesions with a central region of complete cell death characterized by diffuse coagulative-type necrosis and an 8 mm radius. A distinct 3 mm-wide transition zone of partial tissue injury surrounded this area. Within the complete cell death area the swine muscle cells displayed shrunken and degenerated cytoplasm with complete loss of nuclear detail and homogenous pale eosinophilic staining (Figure 3). An increased distance between myocytes was documented, because of interstitial edema. Cytoplasmic vacuolization, increased cell roundness with indistinct membranes and loss or irregular thickness of bands of contraction were major morphologic features. The transition zone exhibited less severe injury with a mixture of histologically live and dead cells.

Vascular thrombosis was not documented in the complete cell death zone and the transition zone. Histology of untreated control tissues showed no degenerative changes (Figure 3).

Clinical efficacy

The time required to achieve complete freezing of the keloids was between 5 and 30 minutes, depending on the volume of the scar treated. A significant reduction in objective parameters and alleviation of the subjective complaints were achieved. The average volume of the keloids before treatment being $2.89 \pm 0.69 \text{ cm}^3$ (range 1–6 cm^3) was significantly reduced to $1.17 \pm 0.46 \text{ cm}^3$ (range 0–4 cm^3) 6 months after a single session of intralesional cryosurgery, which represents a volume reduction of 67.4 ± 23 percent ($p < 0.005$; Figures 4 and 5). In addition, the redness score was reduced from 2.90 ± 0.10 before treatment to 0.80 ± 0.32 six months after cryosurgery ($p < 0.007$), the hardness score from 2.90 ± 0.10 to 0.50 ± 0.22 ($p < 0.004$) and the elevation score from 3.00 ± 0.00 before treatment to 1.00 ± 0.10 six months after cryosurgery ($p < 0.006$). No scar recurrence was registered during the 18-month follow-up period.

The patients mentioned a significant reduction of their subjective complaints a few days after the treatment, which persisted during the follow-up period. The itching score before treatment was 2.50 ± 0.34 compared with 1.19 ± 0.37 six months after cryosurgery ($p < 0.023$). The pain score was 2.00 ± 0.44 before treatment and 0.30 ± 0.21 six months after cryosurgery ($p < 0.016$), and the tenderness score was 2.30 ± 0.33 before treatment and 0.40 ± 0.22 six months after cryosurgery ($p < 0.007$).

Clinical safety

The intralesional treatment was generally well tolerated by the patients. Mild pain or discomfort during and after the procedure was easily managed. Neither active bleeding from the penetration points nor infection was documented. A few hours following intralesional cryosurgery a blister was obvious, and after a few days a crust formed and it

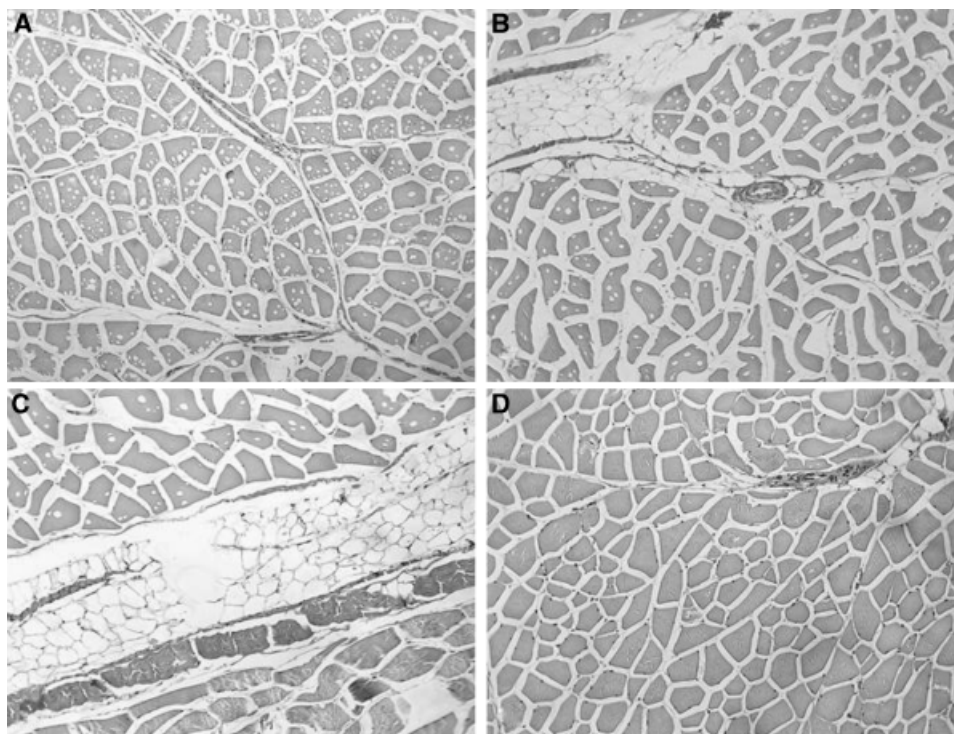


Figure 3. Histological examination of the frozen swine muscle tissue. (A–C) Swine muscle specimen after intralesional cryosurgery. (A) Central region of complete cell death with diffuse cellular nuclear changes as vacuolization of the cytoplasm, irregular bands of contraction, and indistinct membranes. (B) Transitional area showing a mixture of injured and viable myocytes. (C) Note the sharp demarcation between the transitional zone (upper left) and the adjacent normal tissue. (D) In comparison, an untreated specimen (H&E, original magnification $\times 150$).

took 2–3 weeks for the treated scar to heal completely. No adverse reactions, including marked hypopigmentation were registered during the 18-month follow-up period.

Spectral-computerized morphometric analysis, FFT, and fractal analysis of collagen fibers

The spectral-computerized morphometric analysis showed a significant reduction of the ratio between red and green fibers in the keloids before treatment (1.433 ± 0.023) when compared with the data 6 months after treatment (1.610 ± 0.031 , $p < 0.001$).

The FFT algorithm showed that the relative area of collagen fibers in the low-frequency zone was significantly lower in the treated group ($83 \pm 0.7\%$) when compared

with the keloids before treatment ($88 \pm 0.4\%$, $p < 0.001$) (Figures 6 and 7).

The fractal analysis of collagen fibers revealed that the treated scars had a more complex structure. The box dimension method showed a value of 1.740 ± 0.007 of the lesions after treatment when compared with a value of 1.710 ± 0.007 of the keloids before treatment ($p < 0.01$). All these histomorphometric results suggest a more organized architectural pattern of the collagen fibers in the treated scar. A horizontal parallel organization of the collagen fibers in the treated scar was detected being similar to that in the normal dermis, in contrast to the disorientation of the collagen network seen in the keloids before treatment.

DISCUSSION

The response to freezing is a multifactorial injury process.²³ This study confirms a direct cellular injury,³⁷ in which cryoinsult has been proposed to cause protein damage by high solute concentrations created as the cell dehydrates in response to freezing. Protein damage is followed by damage of membrane and enzymatic machinery of the cell in addition to the induction of ice crystals within the cell, which may disrupt the intracellular organelles and plasma membrane.

During cryosurgery, a thermal history profile is created which consists of four stages: cooling rate, end or minimal temperature, hold time (time held at the minimum temperature), and thawing time.³⁸ A slow cooling rate ($10^\circ\text{C}/\text{min}$) causes cell injury due to a sufficient time for osmotic dehydration of the cell, whereas a fast cooling rate ($100^\circ\text{C}/\text{min}$) causes cell injury by the formation of intracellular ice crystals as water is trapped within the cell.

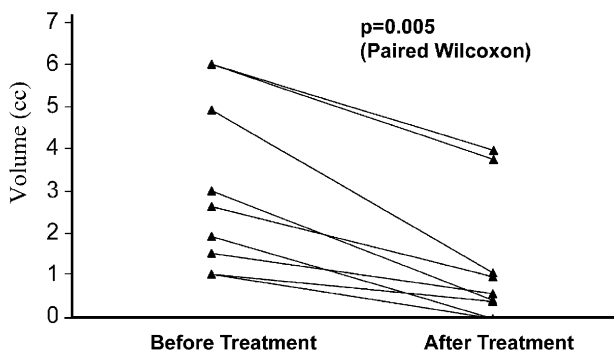


Figure 4. Reduction of scar volume is achieved after a single intralesional cryosurgery session.

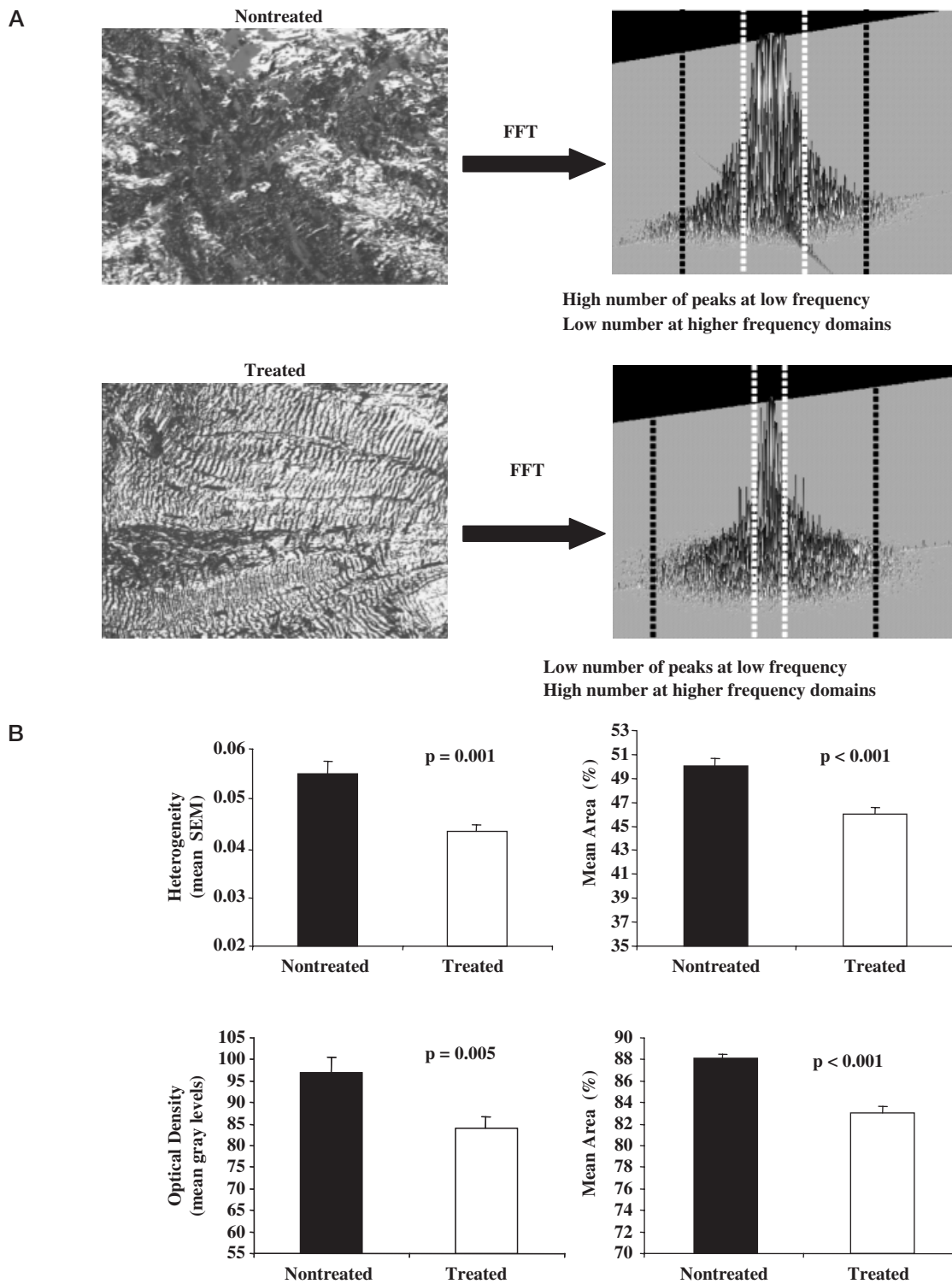


Figure 7. FFT analysis of lesions before and after cryosurgery. (A) 3D fractal power plot views of FFT before and after the treatment with the intralesional cryosurgery technique. Normalization of the treated scar tissue is evident. (B) Comparison of the FFT parameters of heterogeneity and optical density between the nontreated and treated specimens.

supporting direct cryothermic injury as a primary mechanism. Furthermore, the histologic changes observed in adjacent area of the central cryolesion were minimal, revealing a limited demarcated irreversible cell injury. This may explain the absence of hypopigmentation observed in our clinical study. As such, intralesional cryosurgery may occupy an important position in the treatment of black and pigmented-skin populations, which present a high prevalence of keloids and who may benefit from a lower rate of postcryosurgery skin hypopigmentation.

The contact probe showed a different temperature history *ex vivo*. The surface temperature reached -50°C after 30 seconds, -60°C after 60 seconds, and -70°C after 100 seconds. The cooling and thawing rates and the end temperature, including the 3 and 6 mm deep measurements, were faster when compared with the intralesional cryoprobe. The contact probe is composed of brass, thus the similar end temperatures of the isolated contact probe and that in the *ex vivo* studies may be explained by the different metal conductivity when compared with the stainless-steel metal intralesional cryoprobe. In addition the 3 mm deep thermocouple, measured 10°C after 30 seconds, -10°C after 60 seconds, and -25°C after 100 seconds. Thus, the lethal surface temperature, which is far colder than the intralesional cryoprobe, causes an undesirably pronounced superficial cellular and tissue necrosis including the melanocytes with less harm in the deeper layers. This is the reason why the application of the contact probe to the keloid has been limited 30–60 seconds exposures and the total effect of the cryoprobe to the core of the keloid is suboptimal, necessitating repeated treatment sessions.²⁸

The possibility to have a long hold time in the deep scar core, where cryonecrosis is required, employing the intralesional cryoprobe and causing minimal damage to the superficial tissue and melanocytes, has a paramount importance in the clinical application of cryosurgery in treating keloids. In contrast, the lethal zone, which is created by the contact probe, includes the epidermis, upper dermis, and melanocytes, causing a clinically permanent hypopigmentation. This ability of contact cryosurgery to cause hypopigmentation has been applied to lentigo simplex and actinic lentiginos achieving a good aesthetic result without scarring.^{44,45} These experimental findings corroborate our previous clinical results, i.e., the significant reduction in scar volume of 50 percent following a single session,²⁷ which are superior to the clinical results achieved by the contact cryosurgery or the hypodermic needle technique.^{24–26,28} Given this advantage, it is assumed that fewer treatment cycles in order to achieve an optimum result will be necessary.

Histomorphometric examinations have shown a significant tendency toward normalization of the keloid collagen structure as well as the presence of young normal collagen fibers, as previously detected.²⁸ Furthermore, cryotherapy has been found to modify collagen synthesis and differentiation of keloidal fibroblasts *in vitro* toward a normal phenotype.⁴⁶ These findings explain the absence of recurrence after cryosurgery of keloids independent of the technique administered^{24,27} and corroborates cryosurgery as the treatment method of choice for hypertrophic scars and keloids.

In conclusion, this simple-to-operate intralesional cryoprobe technique can be applied to every scar shape and

contour with a sufficient volume at the ear helix and lobe, and may be added to the armamentarium of methods which treat auricular keloids but probably keloids in other localizations, too. There is no need for control of freezing time because the treatment ends when the lesion becomes completely frozen. The major advantage of the intralesional cryoprobe to destroy the deeply localized target tissue with minimal effect on the superficial skin layers may have a significant importance in the clinical application of cryosurgery not only in the treatment of keloids but also of other deeply localized skin lesions and tumors. In addition, the marked efficacy of a single intralesional cryosurgery session presented is another major advantage in comparison with the repeated sessions of standard contact cryosurgery required. From the technical point of view, the presented intralesional cryoprobe technique is safe to use, consumes less cryofluid when compared with the open cryosystems, enables the physician to freeze any keloid to an adequate depth, and it can be associated with any pre-existing cryosurgical unit.

ACKNOWLEDGMENTS

The work was supported by a grant of the Charité University Medicine Berlin to C. C. Z. and a sabbatical leave grant of the Bruce Rappaport Faculty of Medicine, Technion, Israel Institute of Technology to Y. H.-S.

REFERENCES

1. Cosman B, Wolff M. Correlation of keloid recurrence with completeness of local excision. A negative report. *Plast Reconstr Surg* 1972; 50: 163–6.
2. Lawrence WT. Treatment of earlobe keloids with surgery plus adjuvant intralesional verapamil and pressure earrings. *Ann Plast Surg* 1996; 37: 167–9.
3. Mall JW, Pollmann C, Müller JM, Büttemeyer R. Keloidbildung des Ohr läppchens nach Ohrlochstechen. *Chirurg* 2002; 73: 514–6.
4. Russell R, Horlock N, Gault D. Zimmer splintage: a simple effective treatment for keloids following ear piercing. *Br J Plast Surg* 2001; 54: 509–10.
5. Simplot TC, Hoffman HT. Comparison between cartilage and soft tissue ear piercing complications. *Ann J Otolaryngol* 1998; 19: 305–10.
6. Child FJ, Fuller LC, Higgins EM, Du Vivier AWP. A study of the spectrum of skin disease occurring in a black population in south-east London. *Br J Dermatol* 1999; 141: 512–7.
7. Slobodkin D. Why more keloids on back than on front of earlobe. *Lancet* 1990; 333: 923–4.
8. O'Toole GA, Milward TM. Fraternal keloid. *Br J Plast Surg* 1999; 52: 408–10.
9. Koonin AJ. The etiology of keloids: a review of the literature a new hypothesis. *S Afr Med J* 1964; 38: 913–6.
10. Ford LC, King DF, Lagasse LD, Newcomer V. Increased androgen binding in keloids: a pre communication. *J Dermatol Surg Oncol* 1983; 9: 545–7.
11. Salasche SJ, Grabski WJ. Keloids of the earlobe: a surgical technique. *J Dermatol Surg Oncol* 1983; 9: 552–6.

12. Panayias S, Kotzabassakis S, Efstratiou J. Bilateral recurrent fleshy keloids of ear-lobes due to ear-piercing. *Internista* 1996; 4: 107–9.
13. Aköz T, Gideroğlu K, Akan M. Combination of different techniques for the treatment of earlobe keloids. *Aesth Plast Surg* 2002; 26: 184–8.
14. Field LM. Subtotal keloid excision – a preferable preventative regarding recurrence. *Dermatol Surg* 2001; 27: 323–4.
15. Lee Y, Minn KW, Baek RM, Hong JJ. A new surgical treatment of keloid: keloid core excision. *Ann Plast Surg* 2001; 46: 135–40.
16. Hatoko M, Kuwahara M, Shiba A, Tada H, Okazaki T, Muramatsu T, Shirai T. Earlobe reconstruction using a subcutaneous island pedicle flap after resection of “earlobe keloid.” *Dermatol Surg* 1998; 24: 257–61.
17. Ollstein RN, Siegel HW, Gillooley JF, Barsa JM. Treatment of keloids by combined surgical excision and immediate postoperative X-ray therapy. *Ann Plast Surg* 1981; 7: 281–5.
18. Chaudhry MR, Akhtar S, Duvalsaint F, Garner L, Lucente FE. Ear lobe keloid, surgical excision followed by radiation therapy: a 10-year experience. *Ear Nose Throat J* 1994; 10: 779–81.
19. Ragoowanski R, Cornes PGS, Glees JP, Powell BW, Moss ALH. Ear lobe keloids: treatment by a protocol of surgical excision and immediate postoperative adjuvant radiotherapy. *Br J Plast Surgery* 2001; 54: 504–8.
20. Shepherd J, Dawber RPR. Historical and scientific basis of cryosurgery. *Clin Exp Dermatol* 1982; 7: 321–8.
21. Mende B. Keloidbehandlung mittels Kryotherapie. *Z Hautkr* 1987; 62: 1348–55.
22. Zouboulis CC, Orfanos CE. Kryochirurgische Behandlung von hypertrophen Narben und Keloiden. *Hautarzt* 1990; 41: 683–8.
23. Zouboulis CC. Principles of cutaneous cryosurgery: an update. *Dermatology* 1999; 198: 111–7.
24. Zouboulis CC, Zouridaki E, Rosenberger A, Dalkowski A. Current developments and uses of cryosurgery in the treatment of keloids and hypertrophic scars. *Wound Rep Reg* 2002; 10: 98–102.
25. Zouboulis CC, Rosenberger AD, Forster T, Beller G, Kratzsch M, Felsenberg D. Modification of a device and its application for intralesional cryosurgery of old recalcitrant keloids. *Arch Dermatol* 2004; 140: 1293–4.
26. Gupta S, Kumar B. Intralesional cryosurgery using lumbar puncture and/or hypodermic needles for large, bulky, recalcitrant keloids. *Int J Dermatol* 2001; 40: 349–53.
27. Har-Shai Y, Amar M, Sabo E. Intralesional cryotherapy for enhancing the involution of hypertrophic scars and keloids. *Plast Reconstr Surg* 2003; 111: 1841–52.
28. Zouboulis CC, Blume U, Büttner U, Orfanos CE. Outcome of cryosurgery in keloids and hypertrophic scars. *Arch Dermatol* 1993; 129: 1146–51.
29. Shepherd J, Dawber RPR. Wound healing and scarring after cryosurgery. *Cryobiology* 1984; 21: 157–69.
30. Rabau MY, Dayan D. Polarization microscopy of picosirius red-stained sections: a useful method for qualitative evaluation of intestinal wall collagen. *Histol Histopathol* 1994; 9: 525–8.
31. Melis P, Noorlander ML, van der Horst CM, van Noorden CJF. Rapid alignment of collagen fibers in the dermis of undermined and not undermined skin stretching with skin-stretching device. *Plast Reconstr Surg* 2002; 109: 674–80.
32. Smith SW. *The Scientist and Engineer Guide to Digital Signal Processing*. 2nd ed. San Diego: California Technical Publishing, 1997.
33. De Vries HJ, Enomoto DN, van Marle J, van Zuijlen PP, Mekkes JR, Bos JD. Dermal organization in scleroderma: the fast Fourier transform and the laser scatter method objectify fibrosis in nonlesional as well as lesional skin. *Lab Invest* 2000; 80: 1281–9.
34. Van Zuijlen PPM, van Leeuwen RTJ, Lamme EN, Coppens JE, van Marle J, Middelkoop E. Assessment of collagen bundle orientation in scar tissue by means of fast Fourier transform and laser scattering. *Wound Rep Reg* 1998; 6: A493. (Abstract).
35. Mandelbrot B. *The Fractal Geometry of Nature*. New York: W.H. Freeman and Co, 1982.
36. Cross SS, Cotton DWK, Underwood JCE. Measuring fractal dimensions: sensitivity to edge-processing functions. *Anal Quant Cytol Histol* 1994; 16: 375–8.
37. Hoffmann NE, Bischof JC. Cryosurgery of normal and tumor tissue in the dorsal akin flap chamber: part I – thermal response. *J Biomech Eng* 2001; 123: 301–9.
38. Hoffmann NE, Bischof JC. The cryobiology of cryosurgical injury. *Urology* 2002; 60 (Suppl. 2A): 40–9.
39. Tatsutani K, Rubinsky B, Onik G, Dahiya R. Effect of thermal variables on frozen human primary prostatic adenocarcinoma cells. *J Urol* 1996; 48: 441–7.
40. Barker JH, Bartlett R, Funk W, Hammersen F, Messmer K. The effect of superoxide dismutase on the skin microcirculation after ischemia and reperfusion. *Prog Appl Microcirculation* 1987; 12: 276–81.
41. Manson PN, Jesudass RJ, Marzella L, Bulkley GB, Im MJ, Narayan KK. Evidence for an early free radical-mediated reperfusion injury in frostbite. *Free Radic Biol Med* 1991; 10: 7–11.
42. Aliev G, Ragazzi E, Smith M, Mironov A, Perry G. Morphological features of regeneration of rabbit aorta endothelium after cryoinduced vascular damage. *J Submicrosc Cytol Pathol* 1999; 31: 495–502.
43. Bellman S, Strombeck JO. Transformation of the vascular system in cold injured tissue of the rabbit’s ear. *Angiology* 1960; 11: 108–25.
44. Almond-Roesler B, Zouboulis CC. Successful treatment of solar lentigines by brief gentle cryosurgery using a Kryomed® device. *Br J Dermatol* 2000; 143: 216–8.
45. Zouboulis CC, Rosenberger AD, Adler Y, Orfanos CE. Treatment of solar lentigo with cryosurgery. *Acta Derm Venereol* 1999; 79: 489–90.
46. Dalkowski A, Fimmel S, Beutler C, Zouboulis CC. Cryotherapy modifies synthetic activity and differentiation of keloidal fibroblasts in vitro. *Exp Dermatol* 2003; 12: 673–81.